Conformational Analysis and Rotational Barriers of Alkyl- and Phenyl-Substituted Urea Derivatives

Vyacheslav S. Bryantsev, Timothy K. Firman, and Benjamin P. Hay*

Chemical Sciences Division, Pacific Northwest National Laboratory, P.O. Box 999, Richland, Washington 99354

Received: September 20, 2004; In Final Form: November 9, 2004

Potential energy surfaces (PES) for rotation about the N−C(sp^3) or N−C(aryl) bond and energies of stationary points on PES for rotation about the C(sp^2)−N bond are reported for methylurea, ethylurea, isopropylurea, *tert*-butylurea, and phenylurea, using the B3LYP/DZVP2 and MP2/aug-cc-pVDZ methods. The analysis of alkylureas reveals cis and (less stable) trans isomers that adopt anti geometries, whereas syn geometries do not correspond to stationary points. In contrast, the analysis of phenylurea reveals that the lowest energy form at the MP2 level is a trans isomer in a syn geometry. The fully optimized geometries are in good agreement with crystal structure data, and PESs are consistent with the experimental dihedral angle distribution. Rotation about the C(sp^2)−N bond in alkylureas and phenylurea is slightly more hindered (8.6−9.4 kcal/mol) than the analogous motion in the unsubstituted molecule (8.2 kcal/mol). At the MP2 level of theory, the maximum barriers to rotation for the methyl, ethyl, isopropyl, *tert*-butyl, and phenyl groups are predicted to be 0.9, 6.2, 6.0, 4.6, and 2.4 kcal/mol, respectively. The results are used to benchmark the performance of the MMFF94 force field. Systematic discrepancies between MMFF94 and MP2 results were improved by modification of several torsional parameters.

Introduction

Urea and its derivatives comprise an important class of organic compounds that have a great variety of applications in fundamental and applied science. The presence of urea or the urea moiety in the products of metabolism of nitrogen-containing compounds[1] and in many biologically important natural compounds (enzymes, nucleotides, vitamin B_{13})[2] makes it the subject of great interest in biochemistry. Other important topics include urea-induced unfolding of proteins in water solutions[3] and the chiral recognition of amino acids by urea-based receptors.[4] In pharmaceutical chemistry, urea-based compounds are highly potent osmotic, antitumor drugs[5] and HIV protease inhibitors.[6] A hydrogen-bonding network of urea-containing moieties is potentially useful for the construction of nonlinear optical devices,[7−9] stable self-assembled monolayers,[10] and for industrially important resins.[11] The use of the lone pair of either oxygen or nitrogen to coordinate with different metal ions makes urea attractive in coordination chemistry.[5,12] Finally, the anion binding properties of urea resulting from its ability to form two hydrogen bonds are also well established. The −HN−C(═O)−NH− unit has been attached to a variety of scaffolds (calix[4]-arene,[13,14] porphyrin,[14,15] ferrocene,[16] tris(ethyl)amine,[17] *cis*-1,3,5-methylcyclohexane,[17b] cholic acid,[18] naphthalene,[19] etc.[20]) and incorporated into macrocycles[21] to produce effective anion receptors.

Knowledge of the shapes and energetics of urea molecules is essential for understanding the rich chemistry of this important functional group. Electronic structure calculations provide a convenient method for obtaining such information. The majority of prior electronic structure calculations, however, have been limited to the study of urea itself.[7,12,22−31] These studies have yielded rotational barriers for the C_a−N bond and have established that local minima for urea are nonplanar. Studies of alkyl-substituted ureas have been less numerous.[23,30,32−36] Barriers have been reported for rotation about the C_a−N bond of mono-, di-, and tetramethylureas at the HF/6-31G* and MP2/6-31G* levels of theory[23,32] and *N*,*N*′-dimethyl-*N*,*N*′-di-1-naphthylurea at the HF/6-31G** level.[33] However, no electronic structure calculations of the potential energy surface (PES) for the rotation of different *N*-alkyl or *N*-aryl groups in urea, apart from the methyl group,[34] have been reported.

In several instances, the data obtained from electronic structure calculations have been used in force field parametrization for modeling the urea functional group. Urea parameters have been reported for the QMFF force field,[38] the MMFF94 force field,[39] and three different variants of the MM2 force field.[23,32,37] In these studies, conformational analysis has focused on the C_a−N bond rotation in a limited number of simple urea derivatives. None of these force field models has been tested extensively for its ability to reproduce the shapes and relative energies of substituted urea derivatives.

Herein we report conformational analyses for urea, methyl, ethyl, isopropyl, *tert*-butyl, and phenylurea, **1**−**6** (Scheme 1), performed with density-functional theory (DFT) and second-order Möller−Plesset perturbation theory (MP2). All possible minima generated by rotation about both C_a−N and N−C(alkyl) or N−C(aryl) bonds have been considered. Fully optimized geometries are in good agreement with crystal structure data, and calculated PESs are consistent with experimental dihedral angle distributions. The results are used to benchmark and improve the performance of one of the existing force field models, MMFF94.

* Corresponding author. Tel: 509/372-6239. Fax: 509/375-4381. E-mail: Ben.hay@pnl.gov.

10.1021/jp0457287 CCC: $30.25
Published on Web 01/11/2005

SCHEME 1

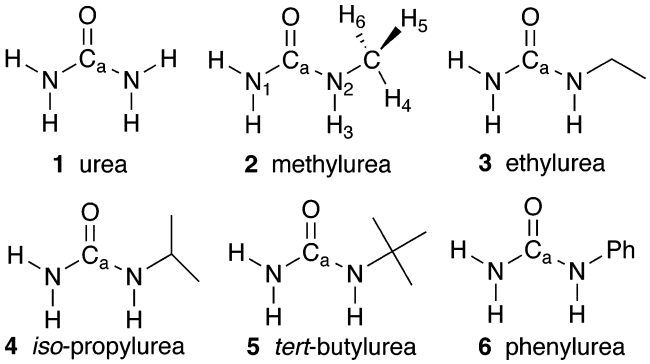

Theoretical Details

Electronic Structure Calculations. Conformational analysis of the alkyl- and phenylureas was performed with the NWChem program[40] using both DFT[41] and second-order Möller−Plesset perturbation theory (MP2).[42] DFT calculations were done with Becke's[43] three-parameter functional and the correlation function of Lee, Yang, and Parr[44] (B3LYP) using a polarized double-ζ basis set (DZVP2) optimized for DFT calculations.[45] No charge fitting was used. MP2 calculations were done using the correlation-consistent aug-cc-pVDZ basis set,[46] including all electrons in the correlation treatment.

The potential energy surfaces, PESs, were obtained by constraining the corresponding dihedral angles (N−C_a−N−X for rotation about the C_a−N bond and C_a−N−C−X for rotation about the N−C bond, where X = H or C) and fully optimizing the remaining internal coordinates. Intervals of 15° and 30° were used for B3LYP and MP2 calculations, respectively. Additional calculations in 5° increments were performed around maxima. The approximate location of stationary points on the PES was found, and full geometry optimization of the minimum energy and transition state structures for rotation about the C_a−N bond was performed at the B3LYP level of theory. The B3LYP geometries were used as starting points for full optimization of geometrical parameters at the MP2/aug-cc-pVDZ level. Frequencies were computed analytically at the B3LYP level to characterize each stationary point as a minimum or a transition state.

Cambridge Structural Database. Experimental average X-ray diffraction crystal structure parameters and distribution of dihedral angles were obtained through analysis of the Cambridge Structural Database (CSD). The CSD program QUEST[47] was used to identify structures in which at least one of the urea nitrogen atoms is substituted by both a hydrogen atom and an alkyl or phenyl group. Searches yielded 49 methyl, 55 CH_2CH_2X (X is an arbitrary group), 25 isopropyl, 25 *tert*-butyl, and 76 phenyl derivatives of urea when applying constraints of an *R* factor less than 10%, no errors, and no disorder. A statistical analysis of the geometric parameters in these structures was carried out with the CSD VISTA program.[47]

Force Field Calculations. The calculations were performed using the MMFF94 force field[39] implemented in PCMODEL molecular modeling software.[48] Comparison of the MP2 results with those obtained from the default MMFF94 model revealed several discrepancies. MMFF94 overestimates both the barrier heights for rotation about C_a−N bonds and the relative energies between the cis and trans forms for all cases examined, **1**−**6**. In addition, while MMFF94 does a good job at reproducing the N−C(alkyl) rotational PESs, the barrier heights for N−C(aryl) rotation in **6** are greatly overestimated.

TABLE 1: Modified MMFF94 Torsional Parameters[a]

dihedral angle	atom types				V_1	V_2	V_3
N−C_a−N−H	10	3	10	28	1.800	3.300	0.620
N−C_a−N−C(alkyl)	10	3	10	1	−0.300	3.100	0.000
N−C_a−N−C(aryl)	10	3	10	37	1.000	3.800	0.000
C_a−N−C(aryl)−C(aryl)	3	10	37	37	0.000	3.000	0.000
H−N−C(aryl)−C(aryl)	28	10	37	37	0.000	1.100	0.000

[a] Barrier heights, V_1−V_3, are given in kcal/mol.

The majority of these discrepancies are explained by the use of generalized wildcard parameters for torsional interactions, which depend only on the atom type of the central two atoms.[39] Parameters pertaining to rotation about the C_a−N bond were adjusted to obtain a better fit with MP2 barrier heights and cis/trans relative energies. Parameters pertaining to N−C(aryl) rotation were adjusted to fit the MP2 barrier height and geometries. The modified parameters are presented in Table 1. Calculations performed with this modified parameter set are termed MMFF94+.

Results and Discussion

Conformational aspects for each derivative, **1**−**6**, are discussed in separate sections below. For clarity, the discussion follows the same order in each case: the planarity of the structure, barrier to rotation about the C_a−N bond, the relative stability of cis versus trans configurations, and the conformations formed by rotation about the N−C(substituent) bond. Since rotation about the C_a−N bond has been a major focus of prior studies, plots of these PESs are not presented. However, all stable points on these surfaces were optimized, and the geometries and relative energies are discussed. On the other hand, since PESs for rotation about N−C(substituent) bonds have not been reported previously, plots of these PESs are presented for each case.

Two levels of electronic structure theory were used in these studies: B3LYP/ DZVP2 (hereafter referred to as B3LYP) and MP2/aug-cc-pVDZ (hereafter referred to as MP2). The data obtained from the MP2 calculations were used to check the performance of the default MMFF94 model. Systematic discrepancies between MMFF94 and MP2 relative energies led to the modification of several torsion interaction parameters, yielding an improved model: MMFF94+ (see Table 1). Relative energies for all optimized geometries obtained using different methods are summarized in Table 2. Views of these geometries are provided in the corresponding sections below.

Urea. Prior studies have identified five stable geometries (two ground states and three transition states) for urea, **1**.[26,31] These geometries are defined in Figure 1. All five geometries have been located in the current study, and the MP2 optimized structures are shown in Figure 2. Relative energies are summarized in Table 2.

Considerable effort has focused on whether **1** is planar in the gas phase. Early theoretical calculations[22] and experimental studies of **1** in the solid state[49] predicted a fully planar C_{2v} structure. More recent calculations[24−31] and microwave studies on **1** in the gas phase by Godfrey et al.[25] find that it is nonplanar with NH_2 groups somewhat pyramidal. Two conformations of C_2 (anti form) and C_s (syn form) symmetry with NH_2 groups, pyramidalized on opposite and on the same sides of molecular plane, respectively, were found to be true minima with the former structure slightly more stable.[7,12,25−27,29−30] A planar C_{2v} structure was found to be a second-order stationary point connecting two pairs of conformers.[7,12,25,26,29,30]

In accord with recent calculations,[24−31] we find that there are two minima on the PES of **1** corresponding to anti (C_2

TABLE 2: Relative Energies (kcal/mol) for Geometries of 1−6 at Various Levels of Theory

conformer	DFT	MP2	MMFF94	MMFF94+
1 anti	0	0	0	0
1 syn	1.02	1.06	1.95	1.92
1 plane	1.60	1.54	2.49	2.30
1 TS1	8.04	8.16	10.49	8.13
1 TS2	14.18	13.48	12.52	13.46
1 TS3	1.08	1.08	1.96	1.92
2 cis	0	0	0	0
2 trans	0.93	1.25	2.94	1.25
2 TS1	9.67	9.39	13.60	9.43
2 TS2	15.76	15.35	18.14	15.35
3a cis	0	0	0.27	0.26
3a trans	1.65	2.14	3.17	1.79
3a TS1	10.96	10.93	15.09	10.95
3a TS2	17.50	17.36	19.96	16.83
3b cis		0.56	0.54	0.55
3b trans	1.35	1.53	3.34	1.43
3b TS1	10.01	9.12	13.68	9.50
3b TS2	15.98	14.85	18.47	15.72
3c cis	0.14	0.74	0	0
3c trans	0.95	1.67	3.70	1.42
3c TS1	9.66	9.71	13.26	9.09
3c TS2	15.55	15.41	17.92	15.18
4a cis	0	0	0	0
4a trans	1.67	1.95	3.48	2.16
4a TS1	10.96	10.62	14.48	10.37
4a TS2	17.62	17.23	19.70	16.65
4b cis	0.47	0.39	0.92	0.94
4b trans	1.30	1.29	3.62	1.24
4b TS1	9.68	8.55	13.54	9.35
4b TS2	15.55	14.08	18.35	15.65
4c cis	2.32	1.86	1.37	1.38
4c trans	4.20	4.16	5.50	4.17
4c TS1	11.83	10.49	15.18	11.11
4c TS2	18.14	16.75	20.66	17.52
5 cis	0	0	0	0
5 trans	2.41	2.61	4.82	3.51
5 TS1	9.67	8.68	13.20	9.14
5 TS2	16.12	15.16	19.03	15.96
6 cis	0	0.94	0	0.95
6 trans	0.16	0	2.90	0
6 TS1	9.67	9.06	13.67	9.05
6 TS2	12.09	11.03	13.77	11.81

symmetry) and syn (C_s symmetry) forms, while the planar C_{2v} state containing two imaginary frequencies is a second-order stationary point. The relative energies of the C_s and C_{2v} states at the MP2 level are 1.06 and 1.54 kcal/mol, respectively. These values are reproduced by B3LYP, 1.02 and 1.60 kcal/mol, but overestimated by MMFF94, 1.95 and 2.55 kcal/mol, and by MMFF94+, 1.92 and 2.30 kcal/mol. For comparison, reported

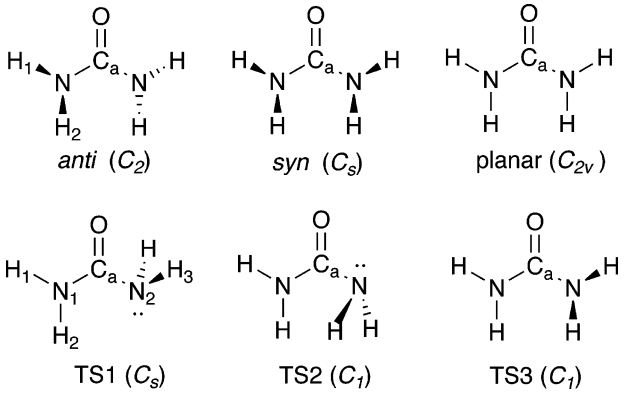

Figure 1. The five known stable points and a second-order saddle point, C_{2v} form, for urea, **1**.

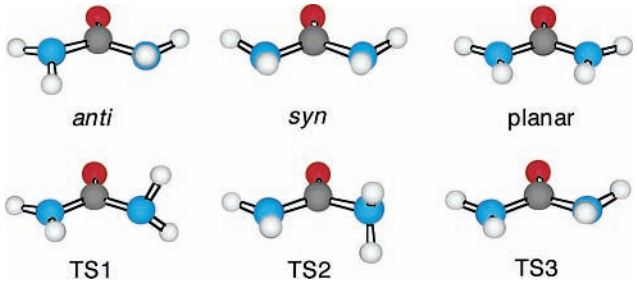

Figure 2. MP2 optimized geometries for **1**.

TABLE 3: Calculated and Experimental Geometric Parameters for the Anti Conformation of 1[a]

feature	DFT	MP2	MMFF94	MMFF94+	expt[b]
C=O	1.228	1.229	1.219	1.219	1.221
C−N	1.395	1.393	1.350	1.350	1.378
$N-H_1$	1.012	1.014	1.013	1.013	1.021
$N-H_2$	1.012	1.014	1.010	1.010	0.998
av. dev[c]	0.012	0.012	0.013	0.013	
O−C−N	123.0	123.2	123.5	123.5	122.6
N−C−N	114.0	113.5	112.9	112.9	114.7
$C-N-H_1$	112.5	112.5	112.8	112.7	112.8
$C-N-H_2$	117.0	116.6	115.4	115.7	119.2
H_1-N-H_2	114.3	114.1	114.2	114.0	118.6
av. dev.	1.6	1.8	2.2	2.3	
$O-C-N-H_1$	13.4	13.8	8.4	9.2	10.8
$O-C-N-H_2$	148.7	148.4	142.1	142.5	156.9
$N-C-N-H_1$	−166.6	−166.2	−171.6	−170.8	−169.2
av. dev.	4.5	4.8	6.5	5.9	

[a] Bond lengths in Å, angles in deg. [b] Experimental data from a microwave study (ref 27). [c] Average absolute deviation between the theoretical and experimental data.

relative energies for the C_s and C_{2v} states are 1.4 and 2.5 kcal/mol for MP2/D95**,[26] 1.20 and 2.73 kcal/mol for MP2/6-311++G**,[25] 0.91 and 1.35 kcal/mol for MP2/6-311G++3df,-3pd,[29] and 0.94 and 1.42 kcal/mol for MP2/aug-cc-pVTZ.[29]

Table 3 summarizes geometrical parameters of the global minimum anti structure of **1**, calculated by various methods, as compared with those obtained from the experimental gas-phase microwave study.[25] The agreement between calculated and experimental structural data is good. All the methods used give structural parameters of similar accuracy although, when compared with the experimental geometry, B3LYP and MP2 calculations yield longer C=O and C−N distances and MMFF94 calculations yield shorter C=O and C−N distances. The modified torsional parameters in MMFF94+ do not noticeably alter bond lengths or angles, but they do have a small influence on the dihedral angles.

Three different transition states (TS) have been identified that connect the anti and syn minima.[26] Rotation about the C_a-N bond gives rise to a C_s symmetry maximum (TS1) and a C_1 symmetry maximum (TS2), where one nitrogen atom is almost or exactly planar and the other nitrogen atom changes its hybridization from a mixture of sp^2 and sp^3 at the minima to a sp^3 state at the TS. TS2 is always higher in energy than TS1 as a result of unfavorable orientation of the lone pair of nitrogen toward the carbonyl oxygen. TS1 and TS2, which involve rotation about the C_a-N bond, are much higher in energy than TS3, which connects the two minima via the inversion of one nitrogen center.

Rotation around the C_a-N bond breaks the conjugation and significantly destabilizes the corresponding TSs. Loss of the conjugation in TS1 and TS2 should lead to substantial elongation of one C−N bond and shortening of another. This is reflected

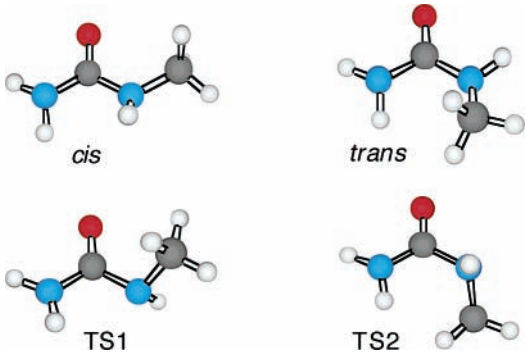

Figure 3. MP2 optimized geometries for **2**.

in B3LYP and MP2 calculations, but the MMFF94 calculations do not reproduce the bond length changes. For example, MP2 gives long and short lengths of 1.455 and 1.363 Å for TS1, whereas MMFF94 gives values of 1.354 and 1.346 Å.

The relative energies for TS1 and TS2 obtained with MP2 and B3LYP (Table 2) are in agreement with reported calculated values of 7.7−9.0 kcal/mol for the lower barrier and 13.5−14.6 kcal/mol for the higher barrier.[7,26,32] The barrier height of 11.0−11.4 kcal/mol[50] measured in solution is several kilocalories per mole above the calculated values. Unfortunately, no experimental values for gas-phase rotational barrier heights have been reported for comparison to the theoretical results. The default MMFF94 model overestimates the barrier height for TS1 and underestimates the barrier height for TS2. This is corrected in MMFF94+.

Inversion at nitrogen to yield TS3 has a much lower barrier height than TS1 and TS2. The relative energy of TS3 is very close to that of the syn form, differing by only 0.02 kcal/mol at the MP2 level. This result is consistent with prior calculations[25,26,29] that predict the difference in energy between the syn form and TS3 to be in the range of 0.02−0.38 kcal/mol, with the most accurate estimate of 0.06 kcal/mol at the MP2/aug-cc-pVTZ level. Such a small barrier height raised an important question of whether the syn form is a distinct conformer or part of a large-amplitude motion of the anti form.[25,29,30]

Methylurea. Methylurea, **2**, exhibits two nonplanar minima, both in an anti configuration with respect to nitrogen pyramidalization. Syn configurations are not stable points on either the B3LYP or MP2 potential surface, consistent with behavior reported for 1,1-dimethylurea.[30] The two minima, designated cis and trans, are interconverted by rotation about the C_a-N bond. As with **1**, there are two TSs for this interconversion analogous to TS1 and TS2 (see Figure 1). The cis, trans, TS1, and TS2 geometries for **2** have been located in the current study, and MP2 optimized structures are shown in Figure 3. Relative energies are summarized in Table 2.

The cis conformation is predicted to be the lowest energy form by all levels of theory. As with **1**, there is good agreement between B3LYP and MP2 relative energies, but the default MMFF94 model overestimates the energy differences. The discrepancies are corrected in MMFF94+.

An NMR study of alkylated ureas in solution shows that only the cis form is present.[51] In addition, a survey of the CSD shows that for every example of urea bearing a methyl substituent, the methyl group adopts the cis configuration with respect to the oxygen atom. Although conformations in solution or in the solid state may be influenced by intermolecular hydrogen-bonding,[26,28] the predicted cis global minimum for **2** is consistent with available experimental data.

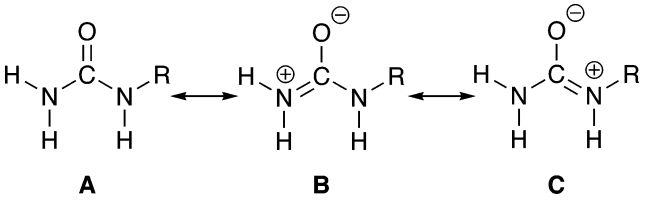

Figure 4. Resonance structures for alkylated urea.

TABLE 4: Calculated and Experimental Geometric Parameters for *cis*-2[a]

feature	DFT	MP2	MMFF94	MMFF94+	expt[b]
$C_a=O$	1.231	1.232	1.220	1.221	1.233 ± 0.011
C_a-N_1	1.402	1.399	1.357	1.357	1.373 ± 0.036
C_a-N_2	1.384	1.385	1.364	1.364	1.337 ± 0.011
$C-N_2$	1.460	1.460	1.441	1.441	1.442 ± 0.014
N_2-H_3	1.011	1.014	1.013	1.013	0.901 ± 0.113
$C-H_4$	1.093	1.097	1.092	1.092	
$C-H_5$	1.097	1.102	1.094	1.094	0.966 + 0.042[c]
$C-H_6$	1.090	1.096	1.094	1.094	
N_1-C_a-O	122.5	123.0	121.9	121.9	121.2 ± 2.0
$N_1-C_a-N_2$	113.9	113.7	111.9	111.9	116.0 ± 1.5
C_a-N_2-C	119.6	117.6	119.6	119.6	121.7 ± 1.0
$C_a-N_2-H_3$	116.0	115.2	113.8	113.8	118.9 ± 3.3
N_2-C-H_4	109.2	108.5	108.6	108.6	
N_2-C-H_5	112.5	112.4	109.0	109.0	110.8 ± 2.1[c]
N_2-C-H_6	108.6	108.8	110.0	110.0	
$O-C_a-N_2-C$	8.9	10.0	5.2	6.6	0 ± 2.4 (0−8.6)[d]
$O-C_a-N_2-H_3$	157.0	153.3	150.1	151.3	180 ± 5.8 (155−180)[d]
γN_1	341.5	341.0	341.4	340.8	
γN_2	352.2	349.2	350.2	350.2	

[a] Bond lengths in Å, angles in deg. Pyramidalization of the nitrogen is expressed in terms of γ, the sum of the three bond angles subtended at nitrogen. [b] Experimental data from X-ray diffraction data for 49 *cis*-methylurea examples. [c] Average data for three methyl hydrogen atoms. [d] Dihedral angles range.

N-Methyl substitution in urea increases the relative energy of TS1 by 1.23, 1.63, 1.08, and 1.30 kcal/mol with MP2, B3LYP, MMFF94, and MMFF94+ methods, respectively (Table 2). Although steric effects on rotational barriers cannot be completely ruled out,[52] this increase in barriers can be rationalized on consideration of urea resonance structures A, B, and C, shown in Figure 4. Contribution from the resonance structure C is expected to increase when R is an electron-donating group. This should result in an increase of the π-bonding character of the $C_a-NH(CH_3)$ bond and in the decrease of the C_a-NH_2 bond order. Experimental barriers for these rotations are available for **2** only in solution,[51] and are approximately 3 kcal/mol higher than calculated ones. Nevertheless, in comparison with **1**, an increase in the barrier height by 1.0 kcal/mol for rotation around the $C-NH(CH_3)$ bond and a decrease in the barrier height for rotation around the $C-NH_2$ bond by 1.5 kcal/mol have been experimentally measured for **2**.[53]

Table 4 summarizes the geometric parameters of the global minimum *cis*-**2**, calculated by various methods. Although experimental gas-phase structural data for **2** are not available, experimental averages from X-ray diffraction data for 49 *cis*-methylurea derivatives are used for comparison with theoretical results. As with **1**, the agreement with the experimental data is good. The average deviation from X-ray bond lengths for heavy atoms is equal to 0.024 Å with B3LYP, 0.023 Å with MP2, and 0.014 Å with MMFF94 and MMFF94+.

Introduction of the weak electron-donating methyl group to **1** results in a slight increase of the $C_a=O$ and C_a-N_1 bond lengths and in a small decrease of the C_a-N_2 bond length, as

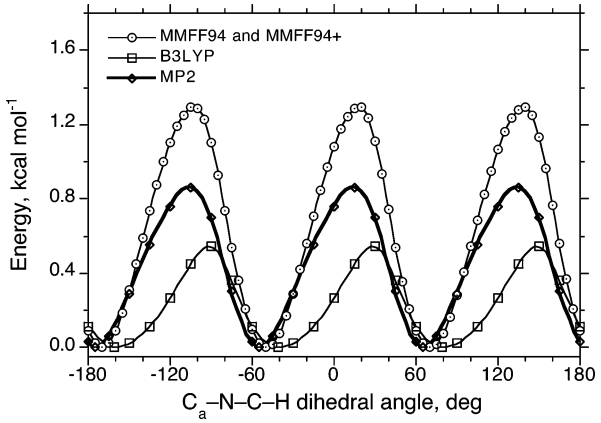

Figure 5. PES for N−C(sp^3) bond rotation in *cis*-**2** at various levels of theory.

predicted by resonance considerations (see C in Figure 4). Note that the sum of the three bond angles (γN_2) around the methylated nitrogen is 9−11° larger than that for the NH_2 group (γN_2). The relative flattening of O=C_a−N_2−C and O=C_a−N_2−H_3 dihedral angles is also indicative of the reduced "pyramidality" at the methylated nitrogen.

Figure 5 shows the PESs for the rotation of the methyl group in *cis*-**2** at different levels of theory. All the methods yield three equivalent minima and maxima, though the position of stationary points on the PES and values of barrier heights are somewhat different. The barrier to rotation of the CH_3 group is 0.86 kcal/mol at the MP2 level, 0.54 kcal/mol at the B3LYP level, and 1.28 kcal/mol at the MMFF94 and MMFF94+ levels. The MP2 equilibrium structure (174°) is closer to an ideal staggered conformation (180°) than those obtained from B3LYP (160°), and MMFF94 and MMFF94+ (170°) calculations (values of one of the H−C−N−C_a dihedral angle are given in parentheses).

Figure 6 illustrates the distribution of C_a−N−C−H dihedral angles in crystal structures, plotted as a histogram of the number of occurrences versus the values of dihedral angles. One comment should be made before comparison between theory and experiment. The three-dimensional structure of the anti configuration implies the existence of a pair of enantiomers with opposite orientation of pyramidal amino groups. The PESs for one stereoisomer are shown in Figure 5. The corresponding PESs for the other stereoisomer are equal to the reflection of the PESs shown in Figure 5 through 0°. Experimental structures, due to rapid pyramidal inversion, reflect time-averaged atomic positions. Thus, the structures often appear planar and it is not possible to assign chirality to them. To provide a meaningful comparison with experiment, we have combined the PESs for the two enantiomers to yield a PES in which every point on the surface corresponds to the lower of the two energies for the enantiomers, as shown in Figure 6. Consistent with theoretical results, the experimental data show that the dihedral angle is populated predominantly in the $-60 \pm 30°$, $60 \pm 30°$, and $180 \pm 30°$ regions, where the calculated energies are within 0.3 kcal/mol from the minima.

Ethylurea. Ethylurea, **3**, behavior is similar to that observed in **2**. All minima adopt an anti configuration with respect to nitrogen pyramidalization. Both cis and trans forms exist, with the cis form being the more stable of the two. Rotation about the N−C(ethyl) bond gives rise to three minima for the cis form and three minima for the trans form. For a given ethyl rotamer, the cis and trans forms are interconverted by rotation about the C_a−N bond with two possible transition states. Three cis minima, three trans minima, three TS1, and three TS2 geometries for **3** have been located in the current study, and MP2 optimized structures are shown in Figure 7. Relative energies are summarized in Table 2.

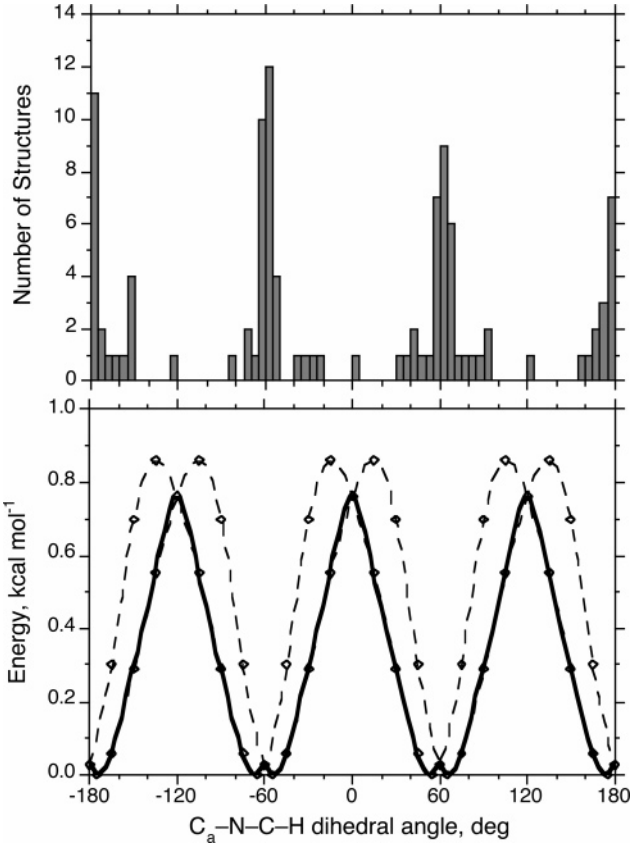

Figure 6. Comparison of the distribution of C_a−N−C−H dihedral angles observed in crystal structures with an MP2 PES (bold line) derived by combining the PESs for the two enantiomers of *cis*-**2** (dashed lines).

For each ethyl rotamer, the cis form is more stable than the corresponding trans form. At the MP2 level, the relative energies of the trans forms are 2.14, 0.97, and 0.93 kcal/mol for **3a**, **3b**, and **3c**, respectively. The result is consistent with experimental data. Analysis of the CSD shows that primary alkyl substituents, $-CH_2CH_2-X$, adopt the cis configuration in 54 of the 55 examples.

The relative energy of the three possible forms of TS1 range from 9.1 to 10.9 kcal/mol with MP2 and from 9.7 to 11.0 kcal/mol with B3LYP. The overestimated range of 13.3 to 15.1 kcal/mol with MMFF94 is corrected to a range of 9.1 to 11.0 kcal/mol with MMFF94+. The variations within a given method result from steric effects associated with the position of the ethyl substituent. Compared with **1**, the lower values of barrier heights, which are similar to those obtained for **2**, reflect electronic (inductive) effects of the attached alkyl group.

A detailed comparison of the geometric parameters at various levels of theory was performed. (A table containing this information is provided as Supporting Information.) Bond lengths and valence angles for **3** are quite similar to those for **2**, and all methods give geometrical parameters of similar accuracy as compared with experimental averages from X-ray diffraction data for *cis*-urea derivatives bearing primary alkyl substituents. The average deviation between the theoretical and experimental bond lengths (heavy atoms) and angles are as follows: MP2 0.021 Å, 2.5°; DFT 0.023 Å, 2.0°; MMFF94 and MMFF94+, 0.015 Å, 2.0°.

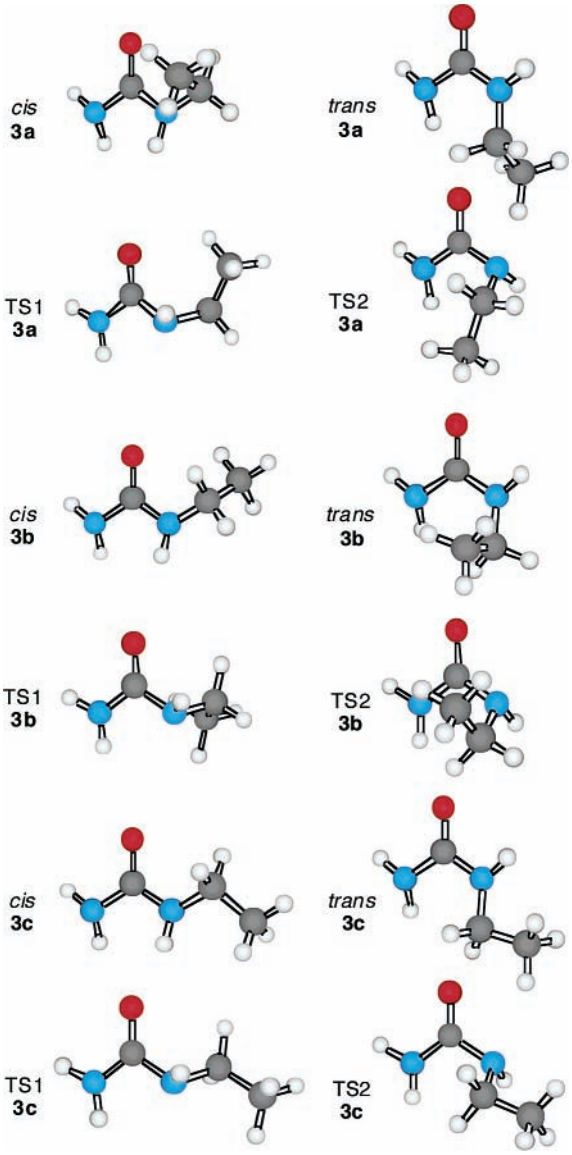

Figure 7. MP2 optimized geometries for **3**.

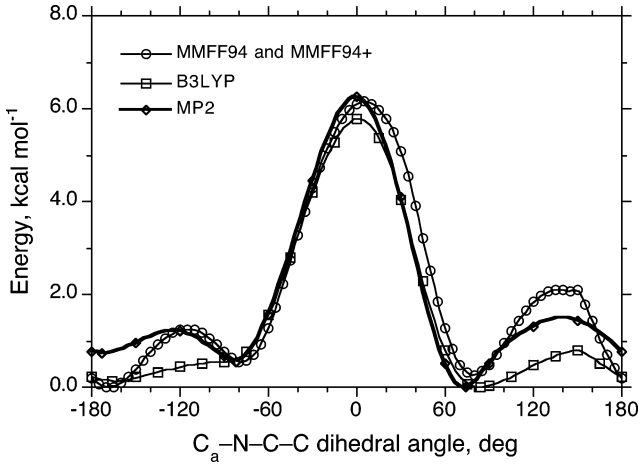

Figure 8. PES for N−C(alkyl) bond rotation in *cis*-**3** at various levels of theory.

Figure 8 shows the PESs for rotation of the ethyl group in *cis*-**3** at different levels of theory. MMFF94 and MMFF94+ give almost identical PESs. The MP2 and MMFF94 methods both yield three minima located approximately ±80°, **3a** and **3b**, and −170°, **3c**. B3LYP, missing the −80° form, yields only two minima. With MP2, the barrier heights are 6.25 kcal/mol at 1°, 1.55 kcal/mol at 139°, and 1.21 kcal/mol at −120°. The asymmetric profile of the PES results from the pyramidal nitrogen atoms. The global minimum near 80°, **3a**, corresponds to a geometry in which the CH_2CH_3 group is staggered with respect to the N−H bond, that is, where one of the H−C−N−H dihedral angles is near 60° (54°, 58°, and 50° with MP2, B3LYP, and MMFF94, respectively). The minimum near −80°, **3b**, is less stable, due to the fact that one of the C−H bonds and the N−H bond adopt a partially eclipsed conformation (H−C−N−H dihedral angle of 11° and 30° with MP2 and MMFF94, respectively).

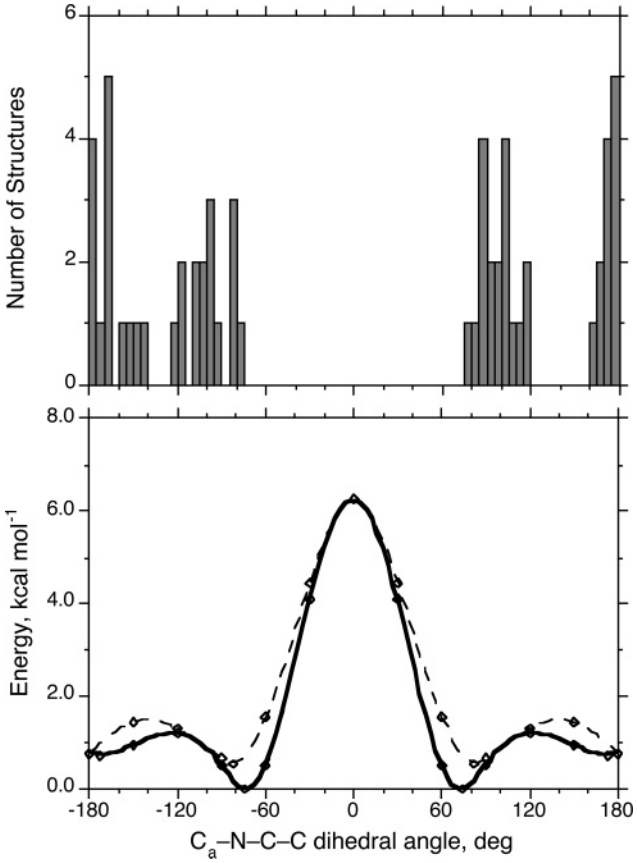

Figure 9. Comparison of the distribution of C_a−N−C−C dihedral angles observed in crystal structures with an MP2 PES (bold line) derived by combining the PESs for the two enantiomers of *cis*-**3** (dashed lines).

X-ray data for 55 examples of CH_2CH_2X substituents (X is any arbitrary group) on urea provide an experimental view of the C_a−N−C−C dihedral angle distribution. This distribution is shown in Figure 9, where it is compared with the MP2 PESs for the two enantiomers of *cis*-**3** (see discussion of **2**). In agreement with the theoretical results, the C_a−N−C−C dihedral angle is populated predominantly in the regions near the calculated minima at ±(90 ± 30°) and 180 ± 20°.

Isopropylurea. Behavior of isopropylurea, **4**, is analogous to that observed for the ethyl derivative, **3**. All minima adopt an anti configuration with respect to nitrogen pyramidalization. Both cis and trans forms exist, with the cis form being the more stable of the two. Rotation about the N−C(ethyl) bond gives rise to three minima for the cis form and three minima for the trans form. For a given isopropyl rotamer, the cis and trans forms are interconverted by rotation about the C_a−N bond with two possible transition states. Three cis minima, three trans minima,

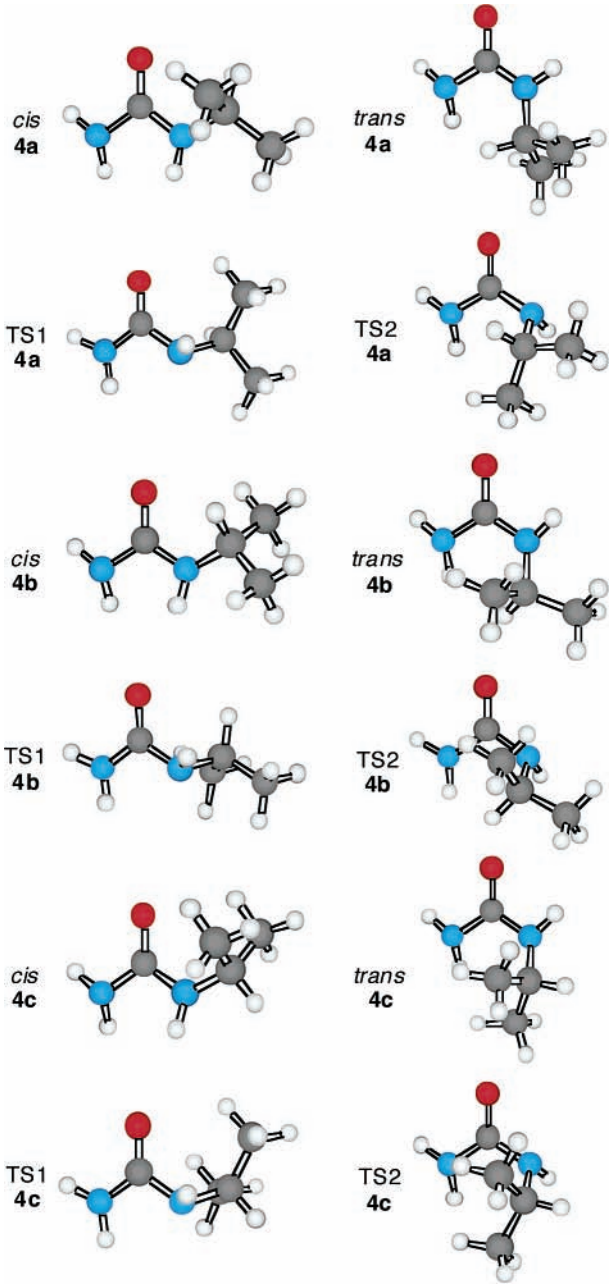

Figure 10. MP2 optimized geometries for **4**.

three TS1, and three TS2 geometries for **4** have been located in the current study, and MP2 optimized structures are shown in Figure 10. Relative energies are summarized in Table 2.

For each isopropyl rotamer, the cis form is more stable than the corresponding trans form. At the MP2 level, the relative energies of the trans forms are 1.95, 0.90, and 2.30 kcal/mol for **4a**, **4b**, and **4c**, respectively. The result is consistent with experimental data. Analysis of the CSD shows that the isopropyl substituent adopts the cis configuration in 23 of the 25 examples.

Barriers to rotation about the C_a-N bond are dependent on the position of the isopropyl group. They range from 8.6 to 10.6 kcal/mol with MP2, 9.7 to 11.8 kcal/mol with B3LYP, 13.5 to 15.2 kcal/mol with MMFF94, and 9.4 to 11.1 kcal/mol with MMFF94+. The lowest barrier height at the MP2 level, 8.55 kcal/mol, is closer to that of **1**, 8.16 kcal/mol, than for **2**, 9.39 kcal/mol. This result is consistent with the experimental observation that the C_a-N rotational barrier of *N*,*N*-dimethylurea, 9.78 kcal/mol,[53] is nearly the same as that observed for *N*,*N*-dimethyl-*N*′-isopropylurea, 9.80 kcal/mol.[54]

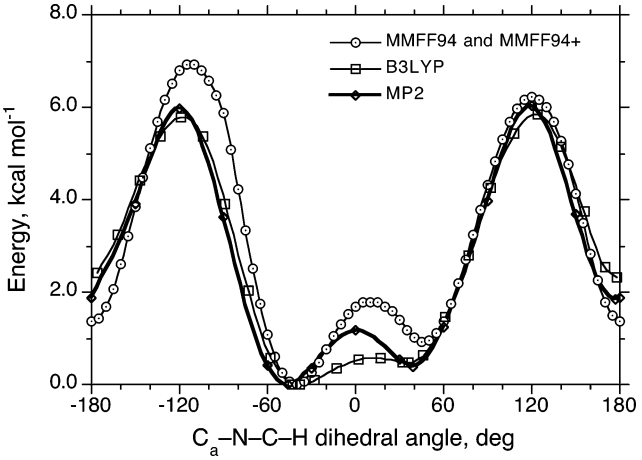

Figure 11. PES for N−C(alkyl) bond rotation in *cis*-**4** at various levels of theory.

A detailed comparison of the geometric parameters at various levels of theory was performed. (A table containing this information is provided in Supporting Information.) Bond lengths and valence angles for **4** are quite similar to those for **2** and **3**, and all methods give geometrical parameters of similar accuracy as compared with experimental averages from X-ray diffraction data for isopropylurea derivatives. The average deviation between the theoretical and experimental bond lengths (heavy atoms) and angles are as follows: MP2 0.018 Å, 1.6°; DFT 0.021 Å, 1.1°; MMFF94 and MMFF94+, 0.018 Å, 1.5°.

Figure 11 shows the PESs for rotation of the isopropyl group in *cis*-**4** at different levels of theory. Here, for reasons of symmetry, the $C_a-N-C-H$ dihedral angle is plotted on the *x*-axis. All calculations yield two minima at about ±40°, **4a** and **4b**, separated by a comparatively low-energy barrier at near 0°, and one high-energy minimum near 180°, **4c**, separated from the other ones by high-energy barriers at about ±120°. As with **3**, the MMFF94 and MMFF94+ models give almost identical PESs. The maximum deviation between MP2 and B3LYP methods is 0.6 kcal/mol at 0°, and between MP2 and MMFF94 methods it is 1.0 kcal/mol at −120°. The global minimum near −40°, **4a**, corresponds to a rotamer where the isopropyl group is staggered with respect to the N−H bond. The local minimum near 40°, **4b**, corresponds to a rotamer where one of the C−C bonds of the isopropyl group is either partially or fully eclipsed with respect to the N−H bond (a H−N−C−C dihedral angle of 13°, 0°, and 23° with MP2, B3LYP, and MMFF94, respectively).

X-ray data for 23 examples of isopropyl-substituted urea derivatives in the cis configuration illustrate the experimental distribution of the $C_a-N-C-H$ angles. This distribution is shown in Figure 12, where it is compared with the MP2 PESs for the two enantiomers of *cis*-**4** (see discussion of **2**). The theoretical results are fully consistent with the experimental distribution. The dihedral angle is populated only in the region between −50° and 50°, where the energy is <1 kcal/mol above the minimum. The higher energy minimum, with a $C_a-N-C-H$ dihedral angle of 180°, has not been experimentally observed.

***tert*-Butylurea.** *tert*-Butylurea, **5**, exhibits one cis minimum and one trans minimum, both in the anti configuration with respect to nitrogen pyramidalization. The cis and trans minima, TS1, and TS2 geometries for **5** have been located in the current

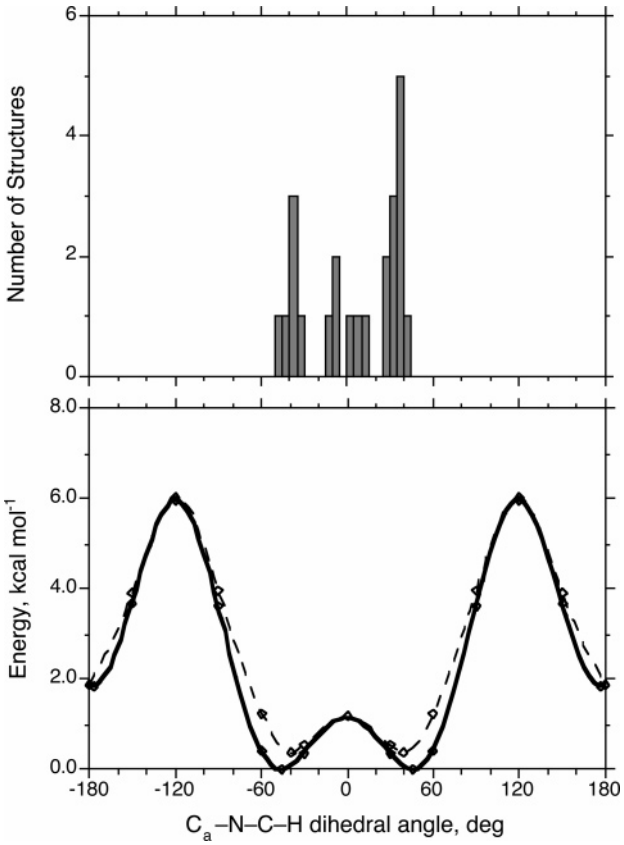

Figure 12. Comparison of the distribution of $C_a-N-C-H$ dihedral angles observed in crystal structures with an MP2 PES (bold line) derived by combining the PESs for the two enantiomers of *cis*-**4** (dashed lines).

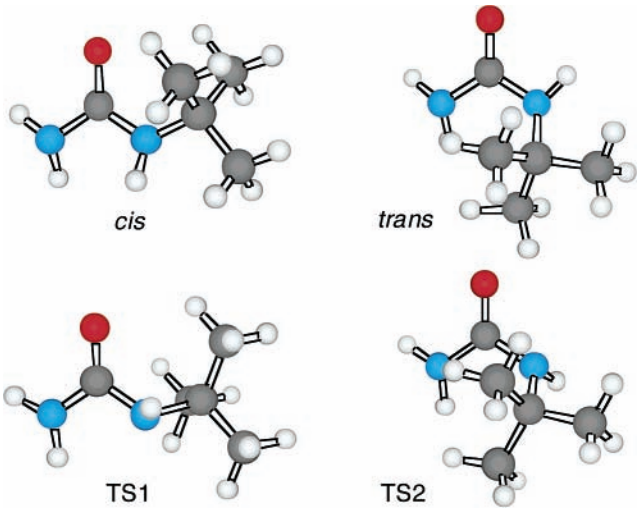

Figure 13. MP2 optimized geometries for **5**.

study, and MP2 optimized structures are shown in Figure 13. Relative energies are summarized in Table 2.

As with the other alkyl-substituted ureas, the cis form is the global minimum. The cis/trans energy difference for the bulky *tert*-butyl group (2.61, 2.41, 4.82, and 3.51 kcal/mol with MP2, B3LYP, MMFF94, and MMFF94+, respectively) is the largest among the alkyl substituents. Examination of the CSD revealed 25 examples in which a *tert*-butyl substituent is attached to the N−H group of urea, all in the more stable cis configuration. The barrier to rotation about the C_a-N bond in **5**, 8.68 kcal/mol with MP2, is similar to that obtained for **4**, 8.55 kcal/mol, at the same level of theory.

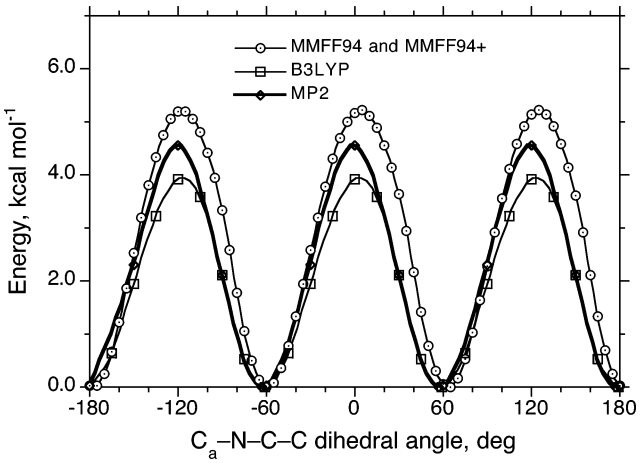

Figure 14. PES for N−C(alkyl) bond rotation in *cis*-**5** at various levels of theory.

A detailed comparison of the geometric parameters at various levels of theory was performed. (A table containing this information is provided in Supporting Information.) Bond lengths and valence angles for **5** are similar to those for **2**−**4**, and all methods give geometrical parameters of similar accuracy as compared with experimental averages from X-ray diffraction data for *tert*-butylurea derivatives. The average deviation between the theoretical and experimental bond lengths (heavy atoms) and angles are as follows: MP2 0.014 Å, 1.2°; DFT 0.018 Å, 0.7°; MMFF94 and MMFF94+, 0.017 Å, 1.7°.

Figure 14 shows the PESs for rotation of the *tert*-butyl group in *cis*-**5** at different levels of theory. All calculations yield 3-fold rotational potentials where the minima occur with methyl groups staggered with respect to the C_a-N bond. As with **2**−**4**, MMFF94 and MMFF94+ yield essentially identical PESs. Three structurally identical minima are located at ±60° and 180°. The barrier to rotation of the *tert*-butyl group is 4.6, 3.9, and 5.2 kcal/mol with MP2, B3LYP, and MMFF94, respectively.

X-ray data for the *tert*-butyl-substituted urea derivatives in the cis configuration illustrate the experimental distribution of the $C_a-N-C-C$ angles. This distribution is shown in Figure 15, where it is compared with the MP2 PESs for the two enantiomers of *cis*-**5** (see discussion of **2**). The theoretical results are fully consistent with the experimental distribution. The dihedral angle is populated at the predicted minima of ±60° and 180°

Phenylurea. Phenylurea, **6**, exhibits one cis minimum and one trans minimum. The cis minimum has an anti configuration and the trans minimum has a syn configuration, with respect to nitrogen pyramidalization. These two minima, TS1, and TS2 geometries for **6** have been located in the current study, and MP2 optimized structures are shown in Figure 16. Relative energies are summarized in Table 2.

Unlike the alkyl-substituted ureas, the relative stability of the two minima depends on the level of theory applied. MP2 and MMFF94+ show the trans form to be more stable than the cis form by 0.94 and 0.95 kcal/mol, respectively. B3LYP and MMFF94 show the cis form to be more stable than the trans form by 0.16 and 2.90 kcal/mol, respectively. The results of recent gas-phase spectroscopic study of **6**, coupled with MP2/6-311++G** single-point calculations on the B3LYP/6-31+G* optimized geometries, suggest that cis and trans conformers have similar relative energies and are both populated thermally.[37] However, examination of the CSD shows that cis form predominates in phenyl-substituted urea derivatives, with the

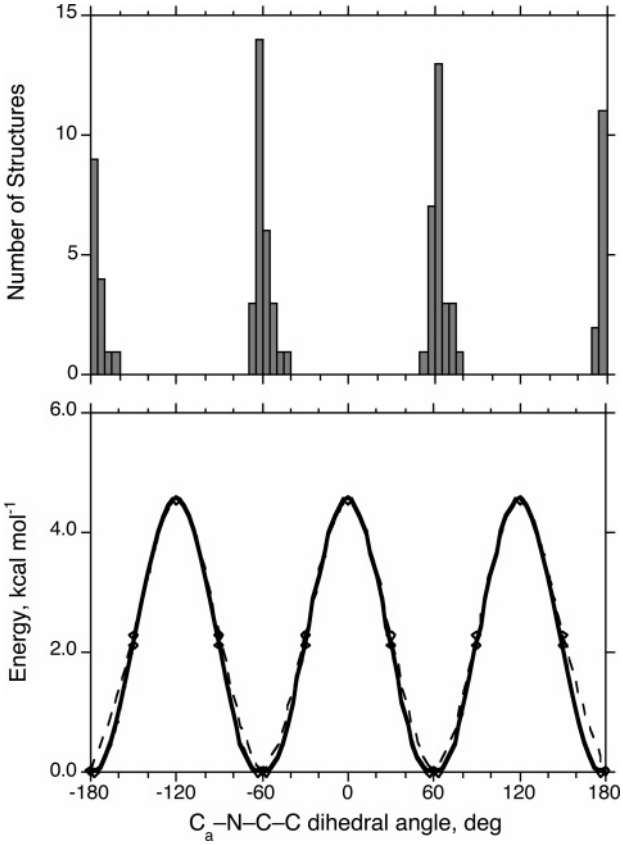

Figure 15. Comparison of the distribution of $C_a-N-C-H$ dihedral angles observed in crystal structures with an MP2 PES (bold line) derived by combining the PESs for the two enantiomers of *cis*-**5** (dashed lines).

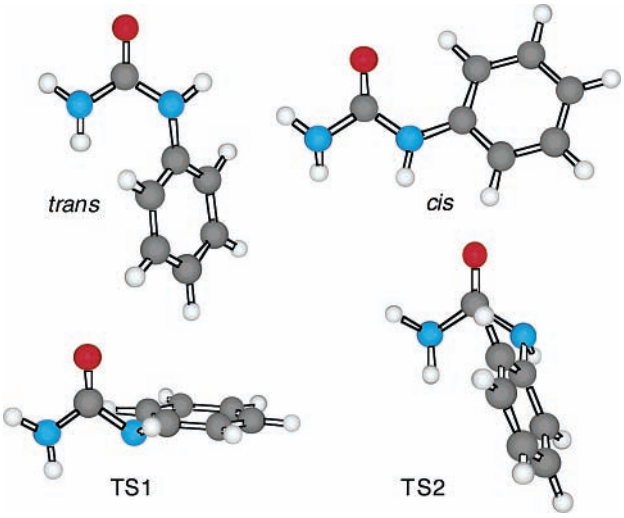

Figure 16. MP2 optimized geometries for **6**.

trans form present in only 1 out of 76 examples. Barriers to rotation about the C_a-N bond are 9.06, 9.67, 13.67, and 9.05 kcal/mol with MP2, B3LYP, MMFF94, and MMFF94+, respectively.

A detailed comparison of the geometric parameters at various levels of theory was performed. (A table containing ths information is provided in Supporting Information.) Bond lengths and valence angles for the cis form of **6** are compared with experimental averages from X-ray diffraction data for phenylurea derivatives. The average absolute deviations for bond lengths and bond angles are as follows: MP2 0.016 Å, 0.7°; B3LYP 0.015 Å, 0.8°; MMFF94 and MMFF94+ 0.010 Å, 1.1°.

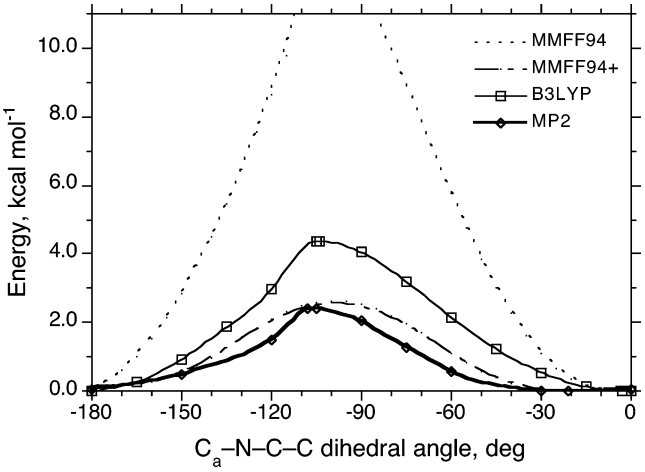

Figure 17. PES for N−C(aryl) bond rotation in *cis*-**6** at various levels of theory.

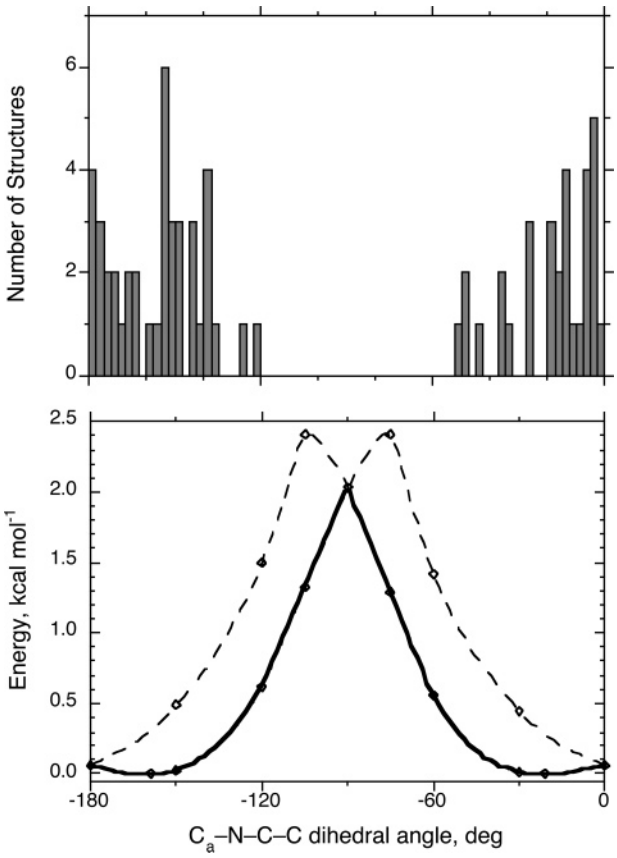

Figure 18. Comparison of the distribution of $C_a-N-C-H$ dihedral angles observed in crystal structures with an MP2 PES (bold line) derived by combining the PESs for the two enantiomers of *cis*-**6** (dashed lines).

Figure 17 shows the PESs for rotation of the phenyl group in *cis*-**6** at different levels of theory. At the MP2 and B3LYP levels, the form of the PES is very similar, but the difference in barrier heights is large, almost 2 kcal/mol, when compared to the behavior of **2**−**5**. The default MMFF94 model gives a very high rotational barrier of about 15 kcal/mol. MMFF94 parameters for two torsional interactions, H−N−C(aryl)−C(aryl) and $C_a-N-C(aryl)-C(aryl)$, were modified to reproduce the MP2 barrier height and the dihedral angle between urea and phenyl planes. Marked improvement was obtained by lowering the 2-fold V_2 parameters for these interactions (see Figure 17).

X-ray data for phenyl-substituted urea derivatives in the cis configuration illustrate the experimental distribution of the $C_a-N-C-C$ angles. This distribution is shown in Figure 18, where it is compared with the MP2 PESs for the two enantiomers of *cis*-**6** (see discussion of **2**). The theoretical results are fully consistent with the experimental distribution. The dihedral angle adopts values in the regions of $0 \pm 60°$ and $180 \pm 60°$, where the calculated energy is less than 1 kcal/mol above the minima.

Conclusions

Exhaustive conformational analyses of urea, **1**, methylurea, **2**, ethylurea, **3**, isopropylurea, **4**, *tert*-butylurea, **5**, and phenylurea, **6**, have been performed with respect to nitrogen pyramidalization and rotation about both C_a-N and N−C(substituent) bonds at the MP2/aug-ccpVDZ and B3LYP/DZVP2 levels of theory. In all cases, fully optimized geometries are in good agreement with available experimental data. In addition, PESs for N−C(substituent) rotation are consistent with the experimental dihedral angle distributions observed in X-ray crystal structures.

The results establish that in contrast to **1**, for which both anti (C_2) and syn (C_s) equilibrium conformations exist, syn forms of mono-alkylureas are not stationary points on either the B3LYP or MP2 potential surfaces. In **2**−**5**, the cis configurations, are more stable than the trans configurations by 0.8 to 2.4 kcal/mol at the B3LYP level and by 0.9 to 2.6 kcal/mol at the MP2 level. Corresponding cis/ trans relative energies, 2.7 to 4.8 kcal/mol, were systematically higher with the MMFF94 model. Rotational barriers around the C_a-N bond for different alkyl substituents are virtually the same at the B3LYP level (9.66−9.68 kcal/mol) and vary slightly at the MP2 level (8.55−9.39 kcal/mol). Corresponding barrier heights calculated by the MMFF94 force field (13.20−13.60 kcal/mol) were systematically greater than those obtained with the electronic structure methods.

Conformational preferences in **6** are dependent on the method applied. At the MP2 level, the trans conformer is predicted to be the global minimum, 0.94 kcal/ mol more stable than the cis conformer. At the B3LYP level, the cis form is the global minimum, 0.16 kcal/mol lower than the trans form. The default MMFF94 force field predicts the cis form to be 2.90 kcal/mol lower than the trans form. In addition, the MMFF94 predicts a very high barrier, about 15 kcal/mol, for rotation of the phenyl group.

We find that the default MMFF94 does an excellent job of predicting the structures of urea derivatives. In addition, with the exception of **6**, examination of PESs for rotation about N−C(substituent) bonds reveals a good correspondence between MMFF94 and MP2 PESs with regard to both relative energies on the PES (error is within ±1 kcal/mol) and the position of minima and maxima. The MMFF94 model fails, however, to reproduce C_a-N rotational barriers and the relative energies of cis and trans forms. It also overestimates the N−C(aryl) rotational barrier. On examination of the default parameter set, these failures were traced to the use of generic torsion parameters. Marked improvement in agreement with the relative energies from MP2 was obtained after simple modification to selected torsion parameters. The modified model, MMFF94+, reproduces MP2 barrier heights for rotation about the C_a-N bond, relative energies of cis and trans forms, and rotational PESs for **2**−**6** to within ≤1 kcal/mol.

Acknowledgment. This work was supported by the Division of Chemical Sciences, Geosciences, and Biosciences, Office of Basic Energy Sciences, U.S. Department of Energy. The research was performed at Pacific Northwest National Laboratory, managed and operated under DOE contract DE-AC06-76RLO-1830 by Battelle Memorial Institute. This research was performed in part using the Molecular Science Computing Facility (MSCF) in the William R. Wiley Environmental Sciences Laboratory, a national scientific user facility sponsored by the Department of Energy's Office of Biological and Environmental Research and located at Pacific Northwest National Laboratory.

Supporting Information Available: Cartesian coordinates and energies (Hartrees) for the MP2/aug-cc-pVDZ, B3LYP/DZVP2, and MMFF94 optimized equilibrium and transition state geometries, and Tables comparing geometric data different levels of theory to that observed in X-ray crystal structures for **3**−**6**. This material is available free of charge via the Internet at http://pubs.acs.org.

References and Notes

(1) Lehninger, A. L.; Nelson, D. L.; Cox, M. M. *Principles of Biochemistry*, 2nd ed.; Worth Publishers: New York, 1993.

(2) (a) Rasmussen, H.; Sletten, E. *Acta Chem. Scand*. **1973**, *27*, 2757. (b) Flippen-Anderson, J. L. *Acta Crystallogr*. **1987**, *C43*, 2228.

(3) (a) Mountain, R. D.; Thirumalai, D. *J. Am. Chem. Soc*. **2003**, *125*, 1950. (b) Smith, L. J.; Berendsen, J. C.; Van Gunsteren, W. F. *J. Phys. Chem. B* **2004**, *108*, 1065.

(4) Kyne, G. M.; Light, M. E.; Hursthouse, M. B.; de Mendoza, J. *J. Chem. Soc., Perkin Trans. 1* **2001**, 1258.

(5) Theophanides, T.; Harvey, P. D. *Coord. Chem. Rev*. **1987**, *76*, 237.

(6) (a) Hodge, C. N.; Lam, P. Y. S.; Eyermann, C. J.; Jadhav, P. K.; Ru, Y.; Fernandez, C. H.; de Lucca, G. V.; Chang, C.-H.; Kaltenbach, R. F., III; Holler, E. R.; Woerner, F.; Daneker, W. F.; Emmett, G.; Calabrese, J. C.; Aldrich, P. E. *J. Am. Chem. Soc.* **1998**, *120*, 4570. (b) Ala, P.; Huston, E.; Klabe, R.; McCabe, D.; Duke, J.; Rizzo, C.; Korant, B.; DeLoskey, R.; Lam, P. Y. S.; Hodge, C. N.; Chang, C.-H. *Biochemistry* **1997**, *36* (7), 1573.

(7) Dixon, D. A.; Matsuzawa, N. *J. Phys. Chem.* **1994**, *98*, 3967.

(8) Manzor, B.; Daly, J. H.; Islam, M. S.; Pethrick, R. A.; Sherwood, J. N. *J. Chem. Soc., Faraday Trans.* **1997**, *93*, 3799.

(9) Halbout, J. M.; Tang, C. L. Properties and Applications of Urea. In *Nonlinear Optical Properties of Organic Molecules and Crystals*; Chemla, D. S., Zyss, J., Eds.; Academic Press: New York, 1987.

(10) Kim, J. H.; Shin, H. S.; Kim, S. B.; Hasegawa, T. *Langmuir* **2004**, *20*, 1674.

(11) Meier, R. J.; Maple, J. R.; Hwang, M.-J.; Hagler, A. T. *J. Phys. Chem.* **1995**, *99*, 5445.

(12) Raptis, S. G.; Anastassopoulou, J.; Theophanides, T. *Theor. Chem. Acc.* **2000**, *105*, 156.

(13) (a) Budka, J.; Lhotak, P.; Michlova, V.; Stibor, I. *Tetrahedron Lett.* **2001**, *42*, 1583. (b) Arduini, A.; Brindani, E.; Giorgi, G.; Pochini, A.; Secchi, A. *J. Org. Chem.* **2002**, *67*, 6188.

(14) Dudic, M.; Lhotak, P.; Stibor, I.; Lang, K.; Proskova, P. *Org. Lett*. **2003**, *5*, 149.

(15) Lee, C.; Lee, D. H.; Hong, J. I. *Tetrahedron Lett.* **2001**, *42*, 8665.

(16) Pratt, M. D.; Beer, P. D. *Polyhedron* **2003**, *22*, 649.

(17) (a) Xie, H. Z.; Yi, S.; Yang, X. P.; Wu, S. K. *New J. Chem*. **1999**, *23*, 1105−1110. (b) Berrocal, M. J.; Cruz, A.; Badr, I. H. A.; Bachas, L. G. *Anal. Chem.* **2000**, *72*, 5295.

(18) (a) Ayling, A. J.; Perez-Payan, M. N.; Davis, A. P. *J. Am. Chem. Soc*. **2001**, *123*, 12716. (b) Sisson, A. L.; Clare, J. P.; Taylor, L. H.; Charmant, P. H.; Davis, A. P. *Chem. Commun.* **2003**, 2246.

(19) Lee, J. Y.; Cho, E. J.; Mukamel, S.; Nam, K. C. *J. Org. Chem.* **2004**, *69*, 943.

(20) (a) Bühlmann, P.; Nishizawa, S.; Xiao, K. P.; Umezawa, Y. *Tetrahedron* **1997**, *53*, 1647−1654. (b) Tobe, Y.; Sasaki, S.; Mizuno, M.; Naemura, K. *Chem. Lett.* **1998**, *8*, 835−836. (c) Albrecht, M.; Zauner, J.; Burgert, R.; Röttele, H.; Fröhlich, R. *Mater. Sci. Eng. C* **2001**, *18*, 185−190. (d) Hoffman, R. W.; Hettche, F.; Harms, K. *Chem. Commun.* **2002**, 782−783. (e) Hettche, F.; Reiss, P.; Hoffman, R. W. *Chem. Eur. J.* **2002**, *8*, 4946−4956. (f) Oh, J. M.; Cho, E. J.; Ryu, B. J.; Lee, Y. J.; Nam, K. C. *Bull. Kor. Chem. Soc.* **2003**, *24*, 1538−1540. (g) Jeon, S.; Park, D. H.; Lee, H. K.; Park, J. Y.; Kang, S. O.; Nam, K. C. *Bull. Kor. Chem. Soc.* **2003**, *24*, 1465−1469. (h) Bondy, C. R.; Gale, P. A.; Loeb, S. J. *J. Am. Chem. Soc.* **2004**, *126*, 5030−5031.

(21) (a) Alcazar, V.; Segura, M.; Prados, P.; de Mendoza, J. *Tetrahedron Lett.* **1998**, *39*, 1033. (b) Ranganathan, D.; Lakshmi, C. *Chem. Commun.* **2001**, 1250.

(22) Vijay, A.; Sathyanarayana, D. N. *J. Mol. Struct.* **1993**, *295*, 245.

(23) Kontoyianni, M.; Bowen, J. P. *J. Comput. Chem.* **1992**, *13*, 657.

(24) Notario, R.; Castano, O.; Herreros, M.; Abboud, J.-L. M. *J. Mol. Struct. (THEOCHEM)* **1996**, *371*, 21.

(25) Godfrey, P. D.; Brown, R. D.; Hunter, A. N. *J. Mol. Struct.* **1997**, *413*−*414*, 405.

(26) Masunov, A.; Dannenberg, J. J. *J. Phys. Chem. A* **1999**, *103*, 178.

(27) Keuleers, R.; Desseyn, H. O.; Rousseau, B.; Van Alsenoy, C. *J. Phys. Chem. A* **1999**, *103*, 4621.

(28) Masunov, A.; Dannenberg, J. J. *J. Phys. Chem. B* **2000**, *104*, 806.

(29) Dobrowolski, J. Cz.; Kolos, R.; Sadlej, J.; Mazurek, A. P. *Vib. Spectrosc.* **2002**, *29*, 261.

(30) Lecomte, F.; Lucas, B.; Gregoire, G.; Schermann, J. P.; Desfrancois, C. *Phys. Chem. Chem. Phys.* **2003**, *15*, 3120.

(31) Bharatam, P. V.; Moudgil, R.; Kaur, D. *J. Phys. Chem. A* **2003**, *107*, 1627.

(32) Strassner, T. *J. Mol. Model.* **1996**, *2*, 217.

(33) Kurth, T. L.; Lewis, F. D. *J. Am. Chem. Soc.* **2003**, *125*, 13760.

(34) Toth, K.; Bopp, P.; Perakyla, M.; Pakkanen, T. A.; Jancso, G. *J. Mol. Struct. (THEOCHEM)* **1994**, *118*, 93.

(35) Galabov, B.; Ilieva, B.; Hadjieva, B.; Dudev, T. *J. Mol. Struct.* **1997**, *407*, 47.

(36) Emery, R.; Macleod, N. A.; Snoek, L. C.; Simons, J. P. *Phys. Chem. Chem. Phys.* **2004**, *6*, 2816.

(37) Berg, U.; Bladh, N. *J. Comput. Chem.* **1996**, *17*, 396.

(38) Maple, J. R.; Hwang, M.-J.; Jalkanen, K. J.; Stockfisch, T. P. *J. Comput. Chem.* **1998**, *19*, 430.

(39) (a) Halgren, T. A. *J. Comput. Chem.* **1996**, *17*, 490. (b) Halgren, T. A. *J. Comput. Chem.* **1996**, *17*, 520. (c) Halgren, T. A. *J. Comput. Chem.* **1996**, *17*, 553. (d) Halgren, T. A.; Nachbar, R. B. *J. Comput. Chem.* **1996**, *17*, 587. (e) Halgren, T. A. *J. Comput. Chem.* **1996**, *17*, 615. (f) Halgren, T. A. *J. Comput. Chem.* **1999**, *20*, 720. (g) Halgren, T. A. *J. Comput. Chem.* **1999**, *20*, 730.

(40) (a) Straatsma, T. P.; Aprà, E.; Windus, T. L.; Bylaska, E. J.; de Jong, W.; Hirata, S.; Valiev, M.; Hackler, M. T.; Pollack, L.; Harrison, R. J.; Dupuis, M.; Smith, D. M. A.; Nieplocha, J.; Tipparaju, V.; Krishnan, M.; Auer, A. A.; Brown, E.; Cisneros, G.; Fann, G. I.; Fruchtl, H.; Garza, J.; Hirao, K.; Kendall, R.; Nichols, J.; Tsemekhman, K.; Wolinski, K.; Anchell, J.; Bernholdt, D.; Borowski, P.; Clark, T.; Clerc, D.; Dachsel, H.; Deegan, M.; Dyall, K.; Elwood, D.; Glendening, E.; Gutowski, M.; Hess, A.; Jaffe, J.; Johnson, B.; Ju, J.; Kobayashi, R.; Kutteh, R.; Lin, Z.; Littlefield, R.; Long, X.; Meng, B.; Nakajima, T.; Niu, S.; Rosing, M.; Sandrone, G.; Stave, M.; Taylor, H.; Thomas, G.; van Lenthe, J.; Wong, A.; Zhang, Z. *NWChem, A Computational Chemistry Package for Parallel Computers*, Version 4.6; Pacific Northwest National Laboratory: Richland, WA, 2004. (b) Kendall, R. A.; Aprà, E.; Bernholdt, D. E.; Bylaska, E. J.; Dupuis, M.; Fann, G. I.; Harrison, R. J.; Ju, J.; Nichols, J. A.; Nieplocha, J.; Straatsma, T. P.; Windus, T. L.; Wong, A. T. *Comput. Phys. Commun.* **2000**, *128*, 260−283.

(41) (a) Parr, R. G.; Yang, W. In *Density Functional Theory of Atoms and Molecules*; Oxford University Press: Oxford, 1989. (b) *Density Functional Methods in Chemistry*; Labanowski, J. K., Andzelm, J. W., Eds.; Springer-Verlag: New York, 1991.

(42) Moller, C.; Plesset, M. S. *Phys. Rev.* **1934**, *46*, 618.

(43) Becke, A. D. *Phys. Rev. A* **1988**, 38, 3098.

(44) Lee, C. T.; Yang, W. T.; Parr, R. G. *Phys. Rev. B* **1988**, *37*, 785.

(45) Godbout, N.; Salahub, D. R.; Andzelm, J.; Wimmer, E. *Can. J. Chem.* **1992**, *70*, 560.

(46) (a) Dunning, T. H., Jr. *J. Chem. Phys.* **1989**, *90*, 1007. (b) Kendall, R. A.; Dunning, T. H., Jr.; Harrison, R. J. *J. Chem. Phys.* **1992**, *96*, 6796.

(47) (a) Allen, F. H.; Kennard, O.; Taylor, R. *Acc. Chem. Res.* **1983**, *16*, 146. (b) Allen, F. H.; Davies, J. E.; Galloy, J. J.; Johnson, O.; Kennard, O.; Macrae, C. F.; Mitchell, E. M.; Smith, J. M.; Watson, D. G. *J. Chem. Inf. Comput. Sci.* **1991**, *31*, 187. (c) Allen, F. H.; Kennard, O. *Chemical Design Automation News* **1993**, *8*, 31.

(48) PCMODEL v. 8.0 is available from Serena Software, Box 3076, Bloomington, IN 47402-3076.

(49) Swaminathan, S.; Craven, B. M.; McMullan, R. K. *Acta Crystallogr.* **1984**, *B40*, 300.

(50) (a) Walter, W.; Schaumann, E.; Rose, H. *Tetrahedron* **1972**, *28*, 3233. (b) Zhao, Y.; Raymond, M. K.; Tsai, H.; Roberts, J. D. *J. Phys. Chem.* **1993**, *97*, 2910. (c) Drakenberg, T.; Forsen, S. *J. Phys. Chem.* **1970**, *74*, 1.

(51) Martin, M. L.; Filleux-Blanchard, M. L.; Martin, G. J.; Webb, G. A. *Org. Magn. Reson.* **1980**, *13*, 396.

(52) Haushalter, K. A.; Lau, J.; Roberts, J. D. *J. Am. Chem. Soc.* **1996**, *118*, 8891.

(53) Anet, A. F.; Ghiaci, M. *J. Am. Chem. Soc.* **1979**, *101*, 6857.

(54) Stilbs, P. *Acta Chem. Scand.* **1971**, *25*, 2635.